Interchain Hydrogen Bonds in Blend Films of Poly(vinyl alcohol) and Its Derivatives with Poly(ethylene oxide)

Chie Sawatari[†] and Tetsuo Kondo*,[‡]

Faculty of Education, Shizuoka University, 836 Oya, Shizuoka, Japan 422-8529, and Forestry and Forest Products Research Institute (FFPRI), P.O. Box 16, Tsukuba Norin Kenkyu, Ibaraki, Japan 305-8687

ABSTRACT: This article proposes that, in binary blends of PEO with polymers bearing hydroxyl groups, only primary and not secondary hydroxyl groups form interchain hydrogen bonds with the skeletal ether oxygen of PEO. To prove this, PVA, propylated PVA, and two hydroxypropylated PVA derivatives—one with only secondary OH groups and the second with a mixture of primary and secondary OH groups, respectively—were used as one component which was blended with PEO in solution. The above hypothesis was confirmed for the resulting blend films using optical microscopic observations, SALS, WAXD, FTIR, and thermodynamic analyses with DSC. Curiously, this idea of selective hydrogen bonding between primary OH groups and oxygen in PEO may also be a driving force for the inclusion of PEO by α-cyclodextrin (CD) as a host−guest system since the primary OH groups at the C-6 position lie at the narrow end of the α-CD.

Introduction

Polymer blends have been studied to improve the physical properties of the individual components for industrial applications. In addition to opening up the possibilities for the applied field, the miscibility of each component polymer is also of interest and importance. One of the driving forces for thermodynamic miscibility is, for example, interchain hydrogen bonds or van der Waals forces. Recently, because environmental issues for nonbiodegradable polymer wastes have arisen, conventional biodegradable polymers such as cellulose and its derivatives, poly(vinyl alcohol) (PVA), and polyesters have again started to attract attention and interest with a view to altering their inherent properties by various methods. Therefore, these types of polymer blends, where cellulosics or PVA can be included as one of the biodegradable components, are once again being considered as possible candidates for industrial use.

We have, thus far, extensively studied the nature of interchain hydrogen bonds believed to be responsible for the polymer−polymer miscibility interaction in cellulosic blends with synthetic polymers.[1−4] In particular, it was demonstrated by FTIR that in cellulose/PVA blend films the interchain hydrogen bonds were formed mainly between the glucose ring ether oxygen and hydroxyl groups (OH) in PVA while other bonds are also formed between secondary OH at either the C-2 or C-3 position and the OH of the PVA component. This is illustrated schematically in Figure 1. This was in contrast to cellulose/poly(ethylene oxide) (PEO) blend films which were found to involve only interchain hydrogen bonding of the primary OH at the C-6 position in cellulose with the skeletal oxygen of PEO[1] (Figure 1). This behavior indicates either the presence of regioselective favorability in a glucose unit of cellulose or a reaction difference between primary and secondary OH groups with regard to the formation of interchain
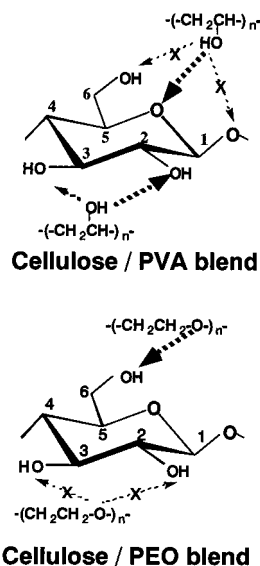
Figure 1. Proposed hydrogen-bonding schemes for the two cellulose/synthetic polymer blend systems, cellulose/PVA and celluose/PEO.

hydrogen bonds in a two-component polymer system. In addition, it has also been reported that phenolic OH groups in poly(*p*-vinylphenol) may form interchain hydrogen bonds leading to miscibility with PEO.[5−8]

Our objective in this article was twofold: first we chose PVA and PEO as the two component polymers for the solution-cast film blend to investigate the role of interchain hydrogen bonding as the driving force for miscibility. With regard to the PVA/PEO blend system, Inamura et al. have previously reported the presence of a liquid−liquid phase separation in the PVA/PEO/water system.[9−11] In contrast, Quintana et al. have described the near total miscibility of PEO with PVA although they did have some reservations about just how complete this miscibility was.[12] In addition, on the basis of our result that only the primary OH in cellulose interacts with the oxygen of PEO, we would predict the immiscibility of PVA, which only has secondary OH,

* To whom correspondence should be addressed.
[†] Shizuoka University.
[‡] FFPRI.

with PEO. Thus, it becomes important to reexamine whether or not PVA/PEO blends are miscible. Second, the two kinds of hydroxypropylated and propylated derivatives of PVA were also synthesized having both of the two possible alcoholic groups, primary and secondary OH, with an appropriate side chain length to mirror the alkyl-blocking effects of the OH groups. These derivatives were then mixed with PEO to determine which produce the most favorable interchain hydrogen bonding with both primary and secondary OH groups.

Experimental Section

Materials. Atactic poly(vinyl alcohol) (PVA) with an average degree of polymerization (DP) of 2000 (M_w: 88 000) and a degree of saponification of 98.9%/mol (Nakarai Tesque Co.) was used after treatment in 40% NaOH solution to remove residual acetyl groups. Poly(ethylene oxide) (PEO), purchased from Wako Pure Chemical Industries Ltd., of a relatively high molecular weight (M_w) ranging from 7000 to 10 000, was employed to avoid any effects of OH groups situated at the end of the molecular chains.[10,13] Gold grade reagents of propylene oxide, propyl iodide, and 2,3-epoxy-1-propanol (glycidol) were purchased from Katayama Chemicals Co. Ltd. HPLC-grade *N,N*-dimethylacetamide (DMAc) (Aldrich Chemical Co., Inc.) was used without further purification.

PVA derivatives were prepared using analogous methods as for cellulose described in previous papers.[14–17] The preparation methods for hydroxypropylated PVA having only secondary OH and for propylated PVA are described as follows. The starting PVA (1.0 g) was dissolved in 80 mL of DMAc under a nitrogen atmosphere at elevated temperatures of 50 °C for 1 h, 70 °C for 1 h, 90 °C for 1 h, and finally 160 °C for 15 min in a tightly capped Erlenmeyer flask. The solution was then cooled to 50 °C with addition of 1 mL of water. Pulverized NaOH (3.6 g) was then added while maintaining the temperature at 50 °C under nitrogen. The required amount of propylene oxide (first 8.9 mL, 1.5 mL × 3 times after 2 h, and then every 1 h) or propyl iodide (first 6.6 mL, 1.1 mL × 3 times after 2 h, and then every 1 h) was then added dropwise in a multiple way depending on the final product. After the last drop of each reagent, the temperature was maintained at 50 °C for the hydroxypropylation and at 70 °C for the propylation. The reaction was then allowed to proceed for 12 h for hydroxylation and 20 h for propylation. Purification techniques for the compounds differed depending on the final product. The hydroxypropylated PVA (HP–PVA) was dissolved in warm water (50 °C) and poured into a dialysis tube for purification. The solution was dialyzed for 1 week and then isolated by freeze-drying. The propylated PVA (Pr–PVA) suspension was poured into water and centrifuged. The resulting precipitate was thoroughly washed and then dissolved in chloroform. Following addition of water and subsequent washing, the chloroform layer was extracted. Finally, the chloroform was removed under reduced pressure at 40 °C until a syrupy material appeared. The propylated polymer, Pr–PVA, was then precipitated by addition of 50% (v/v) aqueous methanol, and it was dried once more under vacuum at 60 °C for 24 h. The degree of substitution (DS) for the OH groups in both polymers prepared from PVA happened to exhibit the same value of 0.79 based on the elemental analysis. Both materials were pastelike, indicating that they were mostly amorphous.

In addition, one other type of hydroxypropylated PVA (HP*–PVA), which contained both primary and secondary OH groups, was prepared according to the method reported for cellulose by Sato et al.[17] with glycidol as the reagent. The DS or molar substitution was 0.8 on the basis of elementary analysis. The density of the synthesized HP*–PVA (1.195 g/cm³) was measured by weighing a glass vial containing a known volume of the well-packed pastelike sample.

Film Preparation. DMAc was used as a common solvent for all samples. Solution concentrations were 0.8 wt % for both PVA and PEO samples. All solutions were filtered and stored in closed containers under a nitrogen atmosphere.

The individual polymer solutions prepared (at 135 °C for 2.5 h for PVA, at 55 °C for HP–PVA and Pr–PVA, and at 55 °C for 120 h stirring for PEO) were mixed in the desired proportions at 75 °C for 24 h. The relative compositions of the two polymers in the mixed solution were 100/0, 75/25, 50/50, 25/75, 20/80, 10/90, and 0/100 (PVA, HP–PVA, or Pr–PVA/PEO) by weight. After stirring at 75 °C for 24 h, blend films were prepared by casting from the mixed solution. One gram of each blended solution was poured onto a flat-bottomed polyethylene tray (Nalgen Co.) at 55 °C and dried at this temperature for 1 week. The DMAc solvent was evaporated to yield an as-cast film. The film was further dried for another week under high vacuum at 55 °C. The films thus produced were then used for wide-angle X-ray diffraction (WAXD), Fourier transform infrared spectroscopy (FTIR), and/or differential scanning calorimetry (DSC) measurements. The films prepared for the FTIR study were sufficiently thin (~10 μm) to obey the Beer–Lambert law.[18]

Measurements. Optical micrographs were obtained using crossed polarizers (Olympus Optical). Small-angle light scattering (SALS) patterns were obtained with a 15 mW He–Ne gas laser (Iwamoto Machine Co. Ltd.) as the light source (wavelength: 632.8 nm). Diffuse surfaces were avoided by sandwiching the specimen between micro cover glasses and using silicone immersion oil having a similar refractive index. WAXD photographs were taken on flat films using nickel-filtered Cu Kα radiation produced by a Rigaku RU-3 X-ray generator at 40 kV and 40 mA. FTIR spectra were obtained with a Perkin-Elmer 1720X FTIR spectrophotometer. Film samples for the FTIR measurements were prepared by casting from DMAc solutions. The wavenumber region investigated ranged from 4000 to 400 cm⁻¹; a total of 32 scans with a 2 cm⁻¹ resolution were signal averaged and stored. Differential scanning calorimetry (DSC) was performed on ca. 4.2 mg of the PEO component in the blends under a nitrogen atmosphere using a Perkin-Elmer DSC-7. The instrument was calibrated with an indium standard. The equilibrium melting point, T_m^{eq}, was determined from DSC measurements as follows: film specimens weighing from 5 to 17 mg each were placed in aluminum sample pans which were then heated to 95 °C and maintained at this temperature for 7 min to eliminate any PEO crystalline residues. The samples were then quenched to the selected isothermal crystallization temperature, T_{ic}, and held at this temperature for 1 h to allow complete crystallization. The samples were then cooled to 20 °C. After each sample was isothermally crystallized, the melting point T_m' was then measured using a heating rate of 10 °C/min. Subsequently by using Hoffman–Weeks plots[19] of the T_m' points thus obtained, an equilibrium melting point (T_m^{eq}) was determined for each film.

Results and Discussion

PVA/PEO Blends as Cast Films. Figure 2 shows cross-polarized optical micrographs of each component—PVA, HP–PVA, Pr–PVA, and PEO—of the homopolymer cast film. PVA and its derivatives exhibited only an almost dark image while the PEO film showed large spherulitic textures of more than 100 μm in diameter.

With increasing of PEO composition in the blend, the opacity of the films in the three systems increased. Optical micrographs for the PVA/PEO blend films (Figure 3) also showed increasing textural details as the PEO composition increased. Even those blends containing less than 25% PEO also displayed some minor textural details. In the 50/50 blend composition, spherulitic textures were barely observed while at the 75/25 PVA/PEO blend composition some relatively small textures, not exactly spherulitic, were observed. This behavior may indicate that phase separation of the two
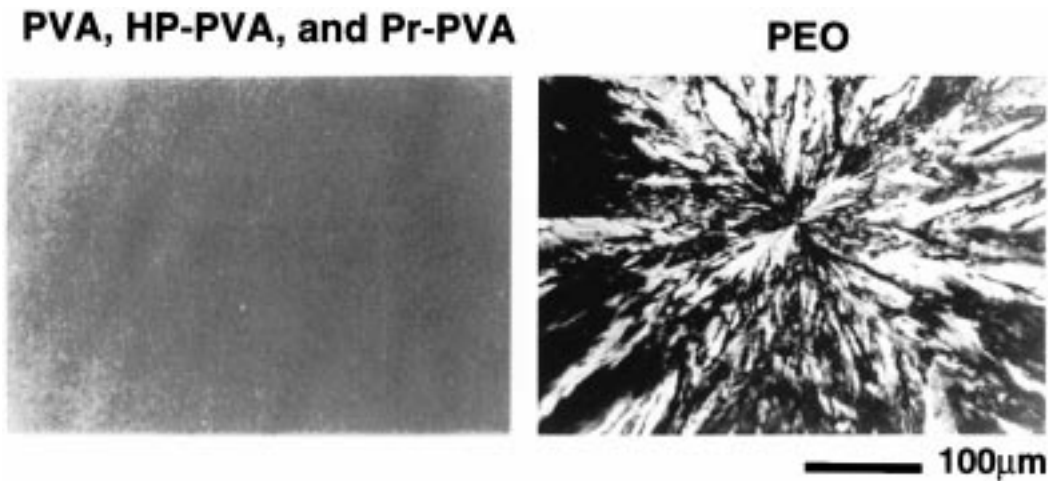
Figure 2. Polarized optical micrographs of PVA and its derivatives and PEO as a cast film.
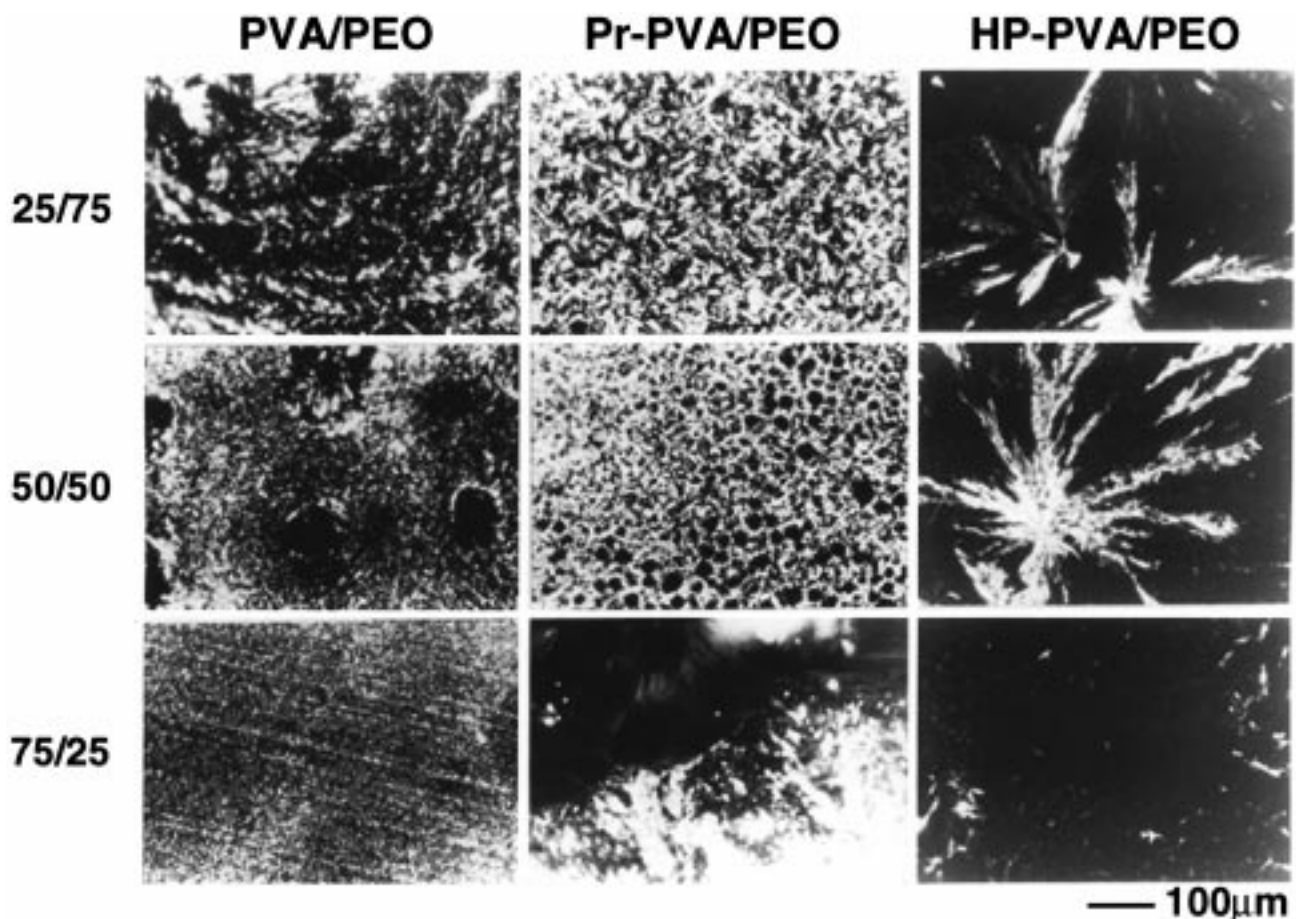
Figure 3. Polarized optical micrographs of a series of PVA or Pr−PVA or HP−PVA blended with PEO.

polymers may arise because of the distribution of PEO crystallites over the PVA amorphous phase in the film. In addition, compatibility, if any, may only start at the 75/25 composition of PVA/PEO. Inamura's article[11] mentions that repulsive interactions may occur in the PVA/PEO/H$_2$O system depending on the PEO content, and it is possible that the minimum repulsive interactions may be present at this composition.

Figure 4 shows Hv light scattering patterns for the two homopolymers and the 50/50 composition blend PVA/PEO film. In the 100/0 composition of PVA (homopolymer) no distinctive scattering from the superstructure was observed. In contrast, the 50/50 blend film exhibited multiple scattering due to disordered lamella textures from growing spherulites of PEO which are hindered by the presence of PVA. This pattern for the 50/50 blend film was also observed in compositions of 75/25 and 25/75. Thus, Hv light scattering patterns did not provide enough of a significant change to be as useful as optical micrographs in distinguishing between the blend compositions. The PEO homopolymer (Figure 4c) exhibited a distinctive four-leaf X-type SALS pattern with azimuthal dependence, indicative of the presence of PEO spherulites, much more clearly than did the above 50/50 blend. Thus, the SALS measurements show a definite diluent effect of PVA in PVA/PEO blends.

PVA/PEO

(a) 100/0

(b) 50/50

(c) 0/100
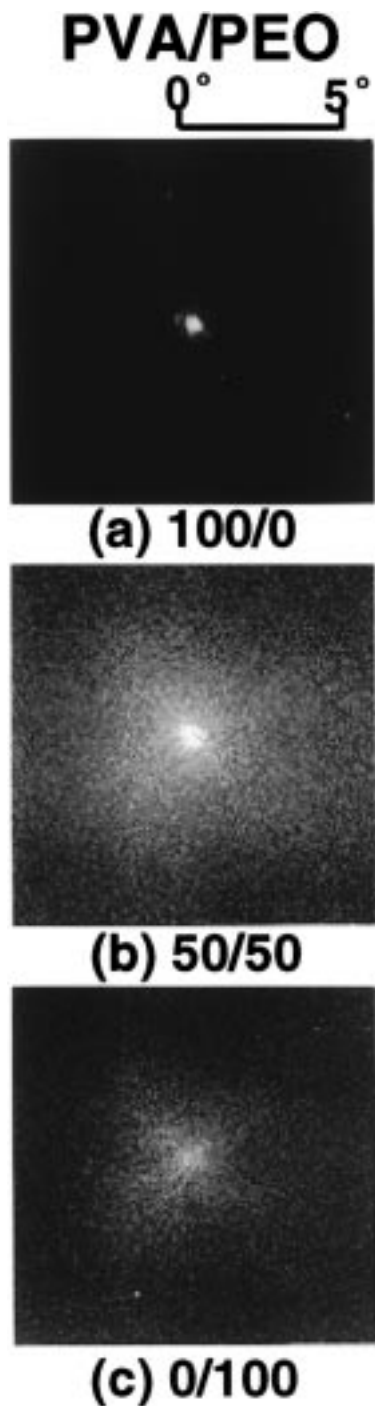
Figure 4. Hv light scattering patterns observed for PVA/PEO blend films.

Figure 5. WAXD patterns of a PVA/PEO (75/25) film and a PVA film obtained from the PVA/PEO film by removal of the PEO.
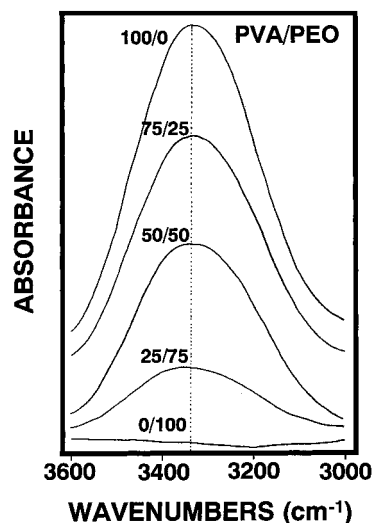
Figure 6. Change of FTIR spectra of PVA/PEO blend films in the range of OH stretching frequencies.

In WAXD photographs of the 75/25 blend film (Figure 5), two typical rings were observed: the outer ring due to the (032) plane of PEO and smaller angle side of the diffraction due to the (120) plane of PEO. Both rings were attributed to PEO because PVA in the blend films appeared to be predominantly amorphous judging from the above optical microscopic observations. However, as the diffraction ring for the (120) plane of PEO overlaps with that for (101) and (10$\bar{1}$) planes of PVA (see Figure 5, PVA only), we could not precisely distinguish which crystallites may contribute to the diffraction ring. Blending the homopolymers did not result in a new diffraction ring, due to cocrystallites, appearing. This would indicate that there was no compatibility of the crystalline domains of the blend film; rather, if compatibility exists it would occur in the amorphous regions.

FTIR analysis was employed to investigate the compatibility of the amorphous regions of PVA/PEO blend films. Since PEO with a relatively high average molecular weight was used to avoid any effect of OH groups at the end of the molecular chains,[10,13] the OH absorption bands contributed by PEO should be negligible in the FTIR spectrum. Thus, the OH absorption bands in the range from 3600 to 3000 cm^{-1} due to the stretching vibration, as shown in Figure 6, were attributed only to OH in PVA which appeared to be highly amorphous. In the FTIR spectra for the various blend compositions, the OH absorption band peak at 3340 cm^{-1} due to inter- or intramolecular hydrogen bonds[20,21] did not shift as the PEO component increased, indicating that the hydrogen bonds in PVA are not affected by blending with PEO. This also indicates that the intermolecular hydrogen bonds were strong enough to maintain their self-assembly in PVA even though it was in a highly amorphous state.

Thus, the results obtained from optical microscopy, SALS, WAXD, and FTIR measurements strongly suggest that PVA is immiscible with PEO in blend films, and each component seems to be able to maintain its individual characteristics.

PVA Derivatives/PEO Blends as Cast Films. *(i) HP− or Pr−PVA/PEO Blends*. Hydroxypropylated

PVA (HP−PVA) with only secondary OH groups and propylated PVA (Pr−PVA) were studied in order to compare their morphological behavior in the presence of PEO with that of PVA alone in PVA/PEO blends. As shown in polarized optical micrographs of Figure 2, both HP−PVA and Pr−PVA yielded dark images similar to that of PVA, indicating that they also both were highly amorphous. Another hydroxypropylated PVA (HP*−PVA) containing a mixture of primary and secondary OH also exhibited similar amorphous behavior. As described previously, PEO cast film exhibited large spherulitic textures, which were more than 100 μm in diameter. Therefore, in the current study of cast films, when the PVA derivatives and PEO were mixed together, it must be assumed to be a blend of amorphous and crystalline polymers in which the miscibility can be evaluated by examining the melting point depression for the PEO crystalline component using the individual equilibrium melting points for the blend films.[2,5,12,19,22−31]

Optical microscopic observations were performed on the blend films prior to FTIR and DSC analysis. The opacity of the blend films increased with increasing PEO composition, as for the PVA/PEO system. Optical micrographs (Figure 3) for the HP−PVA/PEO blend films containing more than 50% of PEO showed large spherulitic textures of more than 100 μm in diameter, which was similar to results for pure PEO. In contrast, only relatively small spherulitic textures were observed at any composition of Pr−PVA/PEO blend films. This suggests that PEO crystallites be distributed within the amorphous phase of the two PVA derivatives in the films, indicating that the two-component polymers could easily be phase separated. In addition, the textures due to PEO crystallites were quite small only in the 75/25 HP−PVA/PEO blend composition, which is similar to the PVA/PEO case where phase separation was assumed to be due to a minimum repulsive interaction between the components as described above. Thus, compatibility for HP−PVA/PEO, if any, may only start occurring at a blend composition of 75/25.

Thermodynamic interactions were also investigated using equilibrium melting point (T_m^{eq}) depressions. Hoffman−Weeks plots[19] of the T_m's for isothermally crystallized PEO were used to obtain T_m^{eq}. Although the T_m^{eq} obtained from the plots were depressed, the depressions were independent of the blend composition in both the HP−PVA/PEO and Pr−PVA/PEO systems, indicating immiscibility. This behavior shows that the secondary OH groups in the HP−PVA do not contribute to interchain hydrogen-bonding interactions with PEO nor are they the driving force for miscibility.

(ii) Interchain Interaction of HP−PVA Having Primary OH Groups with PEO*. In FTIR spectra of HP−PVA/PEO blends, the OH stretching absorption bands were assumed to represent only contributions from OH groups in the highly amorphous HP−PVA component. Figure 7A shows the FTIR spectra for the OH absorption bands with changing PEO content in the HP−PVA/PEO blend. Throughout the entire composition range, the peak maximum at 3400 cm^{-1} due to the secondary OH in the HP−PVA did not change significantly. Only at a blend composition of 75/25 did the peak shape become broader, indicating that some new type of interaction was occurring with the PEO component. This change at the blend composition of 75/25 corresponds to the one noted in the optical micrographs at this same composition. However, at any composition for
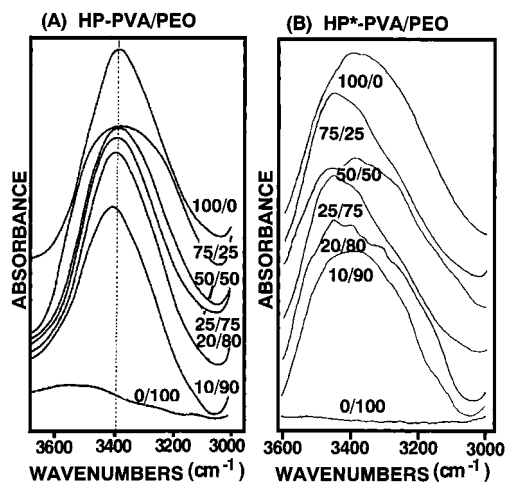
Figure 7. Change of FTIR spectra of (A) HP−PVA/PEO and (B) HP*−PVA/PEO blend films in the range of OH stretching frequencies.
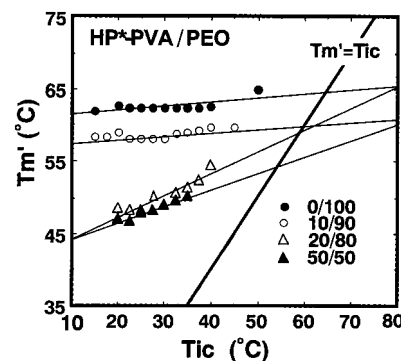
Figure 8. Hoffman−Weeks plots of the melting temperature, T_m', of PEO crystals in the HP*−PVA/PEO blend versus the isothermal crystallization temperature, T_{ic}.

the HP−PVA/PEO blend, the two-component polymers may be considered as immiscible. This also leads to the conclusion that as long as the OH groups involved in bonding are secondary, irrespective of the various side chain lengths involved in the OH, they cannot form hydrogen bonds with PEO. Here in comparing the secondary OH with the primary OH, the HP*−PVA having both primary and secondary OH was used to monitor the change in the OH group frequency in the FTIR spectra for blend films with PEO. As shown in Figure 7B, the behavior of the OH group band depends on the PEO content and was totally different from that exhibited by the HP−PVA/PEO blends. Both the peak maximum and trace shape were changed. In particular, the peak maximum is shifted to higher wavenumbers, as was the case for 2,3-di-*O*-methylcellulose−having only primary OH at the C-6 position−when blended with PEO.[1] Therefore, the above FTIR results allow us to conclude that secondary OH cannot engage in interchain hydrogen bonding with PEO, whereas primary OH may facilitate interchain hydrogen bonding with the skeletal oxygen in PEO.

A thermodynamic investigation was also carried out using equilibrium melting point (T_m^{eq}) depressions obtained from Hoffman−Weeks plots[19] of the T_m's for isothermally crystallized PEO. In contrast to the PVA/PEO blends, the T_m^{eq} depression for the HP*−PVA blend system appeared to be dependent on the blend composition as shown in Figure 8. Since the amorphous HP*−PVA homopolymers exhibited diluent effects in
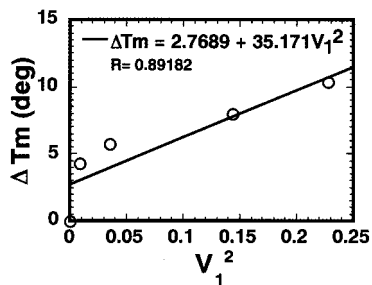
Figure 9. Plot of the melting point depression, ΔT_{m}, versus the square of the volume fraction of the HP*−PVA, $v_1{}^2$, for HP*−PVA/PEO blends.

the blend system, we assumed a change in the chemical potential with increasing amounts of the HP*−PVA components as the PEO melting point decreased in the HP*−PVA blend. The thermodynamic mixing of the two polymers has been dealt by Scott[32] using the Flory−Huggins approximation.[33] The conventional equation for the thermodynamic depression of the melting point caused by a diluent is shown in eq 1:

$$1/T_{\mathrm{m}} - 1/T_{\mathrm{m}}{}^0 = -R(V_{2\mathrm{u}}/\Delta H_{2\mathrm{u}})\{\ln v_2/V_2 + (1/V_2 - 1/V_1)v_1 + Bv_1{}^2/RT_{\mathrm{m}}\} \quad (1)$$

where $T_{\mathrm{m}}{}^0$ is the melting point of PEO and T_{m} is the observed melting point for the blended PEO. In this equation, 1 and 2 refer to HP*−PVA and PEO, respectively. v_1 and v_2 are the polymer volume fractions while V_1 and V_2 are molar volumes. $V_{2\mathrm{u}}$ is the molar volume of the repeat unit of 2, $\Delta H_{2\mathrm{u}}$ is the enthalpy of fusion per mole of the repeat unit of 2, and $v_1{}^2$ is the square of the volume fraction of noncrystallizable component 1 (HP*−PVA).

Since V_1 and V_2 are on the order of ca. 10^4 for HP*−PVA and PEO, the entropy term in eq 1 can be entirely neglected.[23] Equation 1 can then be rearranged into eq 2 where the enthalpic contribution to the melting point depression can be evaluated:

$$\Delta T_{\mathrm{m}} = T_{\mathrm{m}}{}^0 - T_{\mathrm{m}} = -T_{\mathrm{m}}{}^0(V_{2\mathrm{u}}/\Delta H_{2\mathrm{u}})Bv_1{}^2 \quad (2)$$

ΔT_{m} is the melting point depression of the PEO component, and R is the universal gas constant, 1.986 cal deg^{-1} mol^{-1}. Equation 3 relates the B parameter, or interaction energy density characteristic of the two polymers, to the Flory−Huggins interaction parameter, χ_{12}, which describes the enthalpy of mixing:

$$B = RT(\chi_{12}/V_{1\mathrm{u}}) \quad (3)$$

However, there are some morphological effects, which must be taken into account. Specifically, these effects are known to be mainly due to the degree of perfection and the finite size of the crystals.[19] To compensate for these effects, the equilibrium melting points, $T_{\mathrm{m}}{}^{\mathrm{eq}0}$ and $T_{\mathrm{m}}{}^{\mathrm{eq}}$, obtained from the Hoffman−Weeks plots as shown in Figure 8, were used instead of $T_{\mathrm{m}}{}^0$ and T_{m}, respectively, in eq 2. To use the Hoffman−Weeks plots, it is necessary that the PEO component be completely crystallized isothermally. Thus, the $T_{\mathrm{m}}{}^{\mathrm{eq}0}$ and $T_{\mathrm{m}}{}^{\mathrm{eq}}$ were calculated from the Hoffman−Weeks plots using the melting temperatures, $T_{\mathrm{m}}{}'$. In Figure 9 the experimental data for the melting point depression, ΔT_{m}, are plotted versus the square of the volume fraction of the HP*−PVA component, $v_1{}^2$, so that eq 2 can be used. The solid

line was drawn by using a least-squares fitting method assuming that there is a linear relationship between ΔT_{m} and $v_1{}^2$. The volume fraction was calculated using density data for the HP*−PVA (1.195 g/cm^3) and PEO (1.09 g/cm^3) as melt at 75 °C.[34] The measured density value for less packed HP*−PVA was reasonable since it is lower than the density for amorphous PVA which was reported to be 1.26[35] or 1.269[36] g/cm^3. The resulting straight line yielded positive intercepts. Residual entropic effects may be responsible for the nonzero intercept.[2,3,22−30] However, in the present case the low magnitude of the intercepts makes their contribution negligible. From the slopes of the two ΔT_{m} versus $v_1{}^2$ plots, we can assign values to the B parameter and χ_{12} by using eqs 2 and 3 in combination with other known necessary quantities as follows: the heat of fusion per unit volume ($\Delta H_{2\mathrm{u}}/V_{2\mathrm{u}}$) of PEO[37] is 49.7 cal/cm^3, and $V_{1\mathrm{u}}$ = 75.65 cm^3/mol for HP*−PVA. The $V_{1\mathrm{u}}$ value was calculated from the molar masses (90.4 as a DS of 0.8) and the density (1.195 g/cm^3) for HP*−PVA. The slope of the straight line was found to be 35.171°.

From these calculations, the thermodynamic interaction energy density (B is −5.179 cal/cm^3) and parameter (χ_{12} is −0.567 at 75 °C) were obtained. The fairly large negative values for both the B and χ_{12} parameters for HP*−PVA/PEO blends can be explained by the two components interacting thermodynamically in the mixture. The χ_{12} value was also similar in magnitude to that for a cellulose/PEO (χ_{12} is −0.67)[29] system and for a regioselectively methylated 2,3-di-O-methylcellulose/PEO (χ_{12} is −0.51)[2] blend at 75 °C, indicating that interchain hydrogen bonding between the polymer pairs was favorable and involved the primary OH in HP*−PVA and skeletal oxygen in PEO. Such a large negative value for B, which was much larger than those reported previously, was only estimated in the cellulosic blends.[22−27,30] However, it was now possible to determine it quite accurately in the present synthetic polymer pair. Furthermore, these results strongly suggest a general trend showing that favorable interchain hydrogen bonding occurs between primary, rather than the secondary, OH and the skeletal ether oxygen. As for the miscibility of the blend, it can only be considered as partially miscible.

Conclusions

The PVA/PEO blend system was investigated in terms of polymer−polymer interactions to determine its miscibility. We found that, in the blend system, the two polymers appeared to be immiscible on the basis of results obtained from optical microscopic observations, from SALS, and from FTIR. This could and was predicted on results in a previous report[1] on regioselectively substituted methylcelluloses/PEO blends, in which only primary OH at the C-6 position of cellulose was found to be engaged in interchain hydrogen bonding with the skeletal oxygen of PEO. The conclusion to be drawn from these results is that, considering the polymer−polymer interactions possible in blends with PEO, only a second component with primary OH can interact with the skeletal oxygen on PEO. Components having secondary OH cannot interact with this same oxygen group of PEO. Our experimental results for PVA/PEO blends showed an effect of stereohindrance for secondary OH when compared with results for components having primary OH. In attempting to confirm these results, we synthesized two kinds of hydrxypropylated PVA: one

having only secondary OH and one having a mixture of primary and secondary OH. Results proved conclusively that only primary OH could engage in interchain hydrogen bonding with the skeletal oxygen of PEO. Combining this result with previously reported results for 2,3-di-*O*-methylcellulose (23MC)/PEO blends[1,2] leads to the conclusion that the PEO polymer chains are nearly completely included by α-cyclodextrin (α-CD) rings, which have recently attracted attention in host−guest reactions.[38] Specifically, in an analogous fashion as the hydrogen bonds for the 23MC/PEO and HP*−PVA/PEO blends, the C-6 hydroxyl groups, which orient themselves to the inside of the narrow end in the α-CD torus,[39] may engage in interchain hydrogen bonding as a host when it encounters a skeletal oxygen of PEO close enough to act as a guest. These types of inclusion complexes of other polymer chains with CD have also been reported for poly(propylene glycol),[40] poly(iminoo-ligomethylene)s,[41] and poly(viologen).[42] In fact, those cases in aqueous solution were considered to be driven primarily by "hydrophobic interactions".[43] However, we wish to state that, in addition to the possibility of hydrophobic interactions being the driving force for these reactions, it is possible that specific interchain hydrogen bonding between primary OH at the C-6 position of α-CD and the ether oxygen of PEO as an electron donor may also be responsible or contribute to driving these reactions.

References and Notes

(1) Kondo, T.; Sawatari, C.; Manley, R. St. J.; Gray, D. G. *Macromolecules* **1994**, *27*, 210.
(2) Kondo, T.; Sawatari, C. *Polymer* **1994**, *35*, 4423.
(3) Kondo, T.; Sawatari, C. *ACS Symp. Ser.* **1998**, *688*, 296.
(4) Shin, J.-H.; Kondo, T. *Polymer* **1998**, *39*, 6899.
(5) Pedrosa, P.; Pomposo, J. A.; Calahorra, E.; Cortázarm, M. *Polymer* **1995**, *36*, 3889.
(6) Moskala, E. J.; Varnell, D. F.; Coleman, M. M. *Polymer* **1985**, *26*, 228.
(7) Qin, Ch.; Pires, A. T.; Belfiore, L. A. *Polym. Commun.* **1990**, *31*, 177.
(8) Zhang, X.; Takegoshi, K.; Hikichi, K. *Macromolecules* **1992**, *25*, 2336.
(9) Inamura, I.; Toki, K.; Tamae, T.; Araki, T. *Polym. J.* **1984**, *16*, 657.
(10) Inamura, I. *Polym. J.* **1986**, *18*, 269.
(11) Inamura, I.; Jinbo, Y. *Polym. J.* **1991**, *23*, 1143.
(12) Quintana, J. R.; Cesteros, L. C.; Peleteiro, M. C.; Katime, I. *Polymer* **1991**, *32*, 2793.
(13) Martuscelli, E.; Pracella, M.; Yue, W.-P. *Polymer* **1984**, *25*, 1097.
(14) Kondo, T.; Gray, D. G. *J. Appl. Polym. Sci.* **1992**, *45*, 417.
(15) Kondo, T.; Gray, D. G. *Carbohydr. Res.* **1991**, *220*, 173.
(16) Kondo, T. *Carbohydr. Res.* **1993**, *238*, 231.
(17) Sato, T.; Tsujii, Y.; Minoda, M.; Kita, Y.; Miyamoto, T. *Makromol. Chem.* **1992**, *193*, 647.
(18) Coleman, M. M.; Painter, P. C. *J. Macromol. Sci., Rev. Macromol. Chem.* **1978**, *16*, 197.
(19) Hoffman, J. D.; Weeks, J. J. *J. Res. Natl. Bur. Stand., Sect. A* **1962**, *66,* 13.
(20) Krimm, S.; Liang, C. Y.; Sutherland, G. B. B. M. *J. Polym. Sci.* **1956**, *22*, 227.
(21) Tadokoro, H. *Bull. Chem. Soc. Jpn.* **1959**, *32*, 1252.
(22) Nishi, T.; Wang, T. T. *Macromolecules* **1975**, *8*, 909.
(23) Imken, R. L.; Paul, D. R.; Barlow, J. W. *Polym. Eng. Sci.* **1976**, *16*, 593.
(24) Paul, D. R.; Barlow, J. W.; Bernstein, R. E.; Wahrmund, D. C. *Polym. Eng. Sci.* **1978**, *18*, 1225.
(25) Ziska, J. J.; Barlow, J. W.; Paul, D. R. *Polymer* **1981**, *22*, 918.
(26) Martuscelli, E.; Pracella, M.; Yue, W. P. *Polymer* **1984**, *25*, 1097.
(27) Kwei, T. K.; Patterson, G. D.; Wang, T. T. *Macromolecules* **1976**, *9*, 780.
(28) Nishio, Y.; Haratani, H.; Takahashi, T.; Manley, R. St. J. *Macromolecules* **1989**, *22*, 2547.
(29) Nishio, Y.; Hirose, N.; Takahashi, T. *Polym. J.* **1989**, *21*, 347.
(30) Katime, I. A.; Anasagasti, M. S.; Peleteiro, M. C.; Valenciano, R. *Eur. Polym. J.* **1987**, *23*, 907.
(31) Iragorri, J. I.; Cesteros, L. C.; Katime, I. *Polym. Int.* **1991**, *25*, 225.
(32) Scott, R. L. *J. Chem. Phys.* **1949**, *17*, 279.
(33) Flory, P. J. *Principles of Polymer Chemistry*; Cornell University Press: Ithaca, NY, 1953.
(34) Roe, R.-J. *J. Phys. Chem.* **1968**, *72*, 2013.
(35) Wiley, R. *Ind. Eng. Chem.* **1946,** *38*, 959.
(36) Sakurada, I.; Nukushina, K.; Sone, Y. *Kobunshi Kagaku* **1955**, *12*, 506.
(37) Mandelkern, L.; Quinn, F. A.; Flory, P. J. *J. Appl. Phys.* **1954**, *25*, 830.
(38) Harada, A.; Kamachi, M. *Macromolecules* **1990**, *23*, 2821.
(39) Croft, A. P.; Bartsch, R. A. *Tetrahedron* **1983**, *39*, 1417.
(40) Harada, A.; Okuda, M.; Li, J.; Kamachi, M. *Macromolecules* **1995**, *28*, 8406.
(41) Wenz, G.; Keller, B. *Angew. Chem.* **1992**, *104*, 201.
(42) Meier, L. P.; Heule, M.; Caseri, W. R.; Shelden, R. A.; Suter, U. W.; Wenz, G.; Keller, B. *Macromolecules* **1996**, *29*, 718.
(43) Schneider, H.-J. *Angew. Chem.* **1991**, *103*, 1419; *Angew. Chem., Int. Ed. Engl.* **1991**, *30*, 1417.